Melt-electrospinning as a method to improve the dissolution and physical stability of a poorly water-soluble drug

Kristian Semjonov[1], Andres Lust[1], Karin Kogermann[1], Ivo Laidmäe[1], Sirkka Liisa Maunu[4], Sami-Pekka Hirvonen[4], Jouko Yliruusi[3], Gunnar Nurk[2], Enn Lust[2], Jyrki Heinämäki[1]

[1]*Institute of Pharmacy, Faculty of Medicine, University of Tartu, Nooruse 1, 50411 Tartu, Estonia*

[2]*Institute of Chemistry, Faculty of Science and Technology, University of Tartu, Nooruse 1, 50411, Tartu, Estonia*

[3]*Division of Pharmaceutical Chemistry and Technology, Faculty of Pharmacy, Viikinkaari 5E, 00014 University of Helsinki, Finland*

[4]*Department of Chemistry, Faculty of Science, P.O. Box 55, 00014 University of Helsinki, Finland*

Kristian Semjonov
Institute of Pharmacy, Faculty of Medicine, University of Tartu,
Nooruse 1, 50411 Tartu, Estonia
Tel.:+372 51980454
Email: kristian.semjonov@ut.ee

Abstract. The present study introduces a modified melt-electrospinning (MES) method for fabricating the melt-electrospun fibers (MSFs) of a poorly water-soluble drug and carrier polymer. The MES of poorly water-soluble model drug indomethacin (IND) and hydrophilic carrier polymer, Soluplus® (SOL) were prepared at a 1:3 drug-polymer weight ratio. Water was used as an external plasticizer to regulate a MES processing temperature and to improve fiber formation. The fiber size, surface morphology, physical solid state, drug-polymer (carrier) interactions, thermal and chemical stability and dissolution behavior of MSFs were investigated. Solid state nuclear magnetic resonance spectroscopy (NMR) was used to measure T1(^{1}H), and the domain size of IND in MSFs (25-100 nm) was calculated from these results. Solid-state and thermal analysis confirmed the presence of amorphous solid dispersions of IND and SOL. IND was found to be chemically stable during an entire MES process. Only small drug content variability of different MSF batches was detected with high performace liquid chromatography (HPLC). Given findings were verified with the liquid NMR spectroscopy. The dissolution of MSFs was significantly faster than that of physical mixtures (PMs) or pure drug. The enhanced dissolution of MSFs was caused by high surface area, amorphous state of the drug and solubilizing properties of the carrier polymer (SOL).

Keywords: Melt electrospinning, Melt-spun fibers, Poorly water-soluble drug, Indomethacin, Soluplus®, Drug-polymer interactions

1. Introduction

Formulation development of oral solid dosage forms for poorly water-soluble drugs is a major challenge to the pharmaceutical industry (Di et al., 2009). The well-known formulation approaches to tackle this challenge include e.g., salt formation, micronisation, co-crystals, solid dispersions (SDs), surfactants, inclusion complexes with cyclodextrins, and lipid-based systems (Vasconcelos et al., 2007; Williams et al., 2013). Another novel emerging method that enables to formulate poorly water-soluble drugs is electrospinning (ES) of active pharmaceutical ingredient (API) together with an amphiphilic polymer**.**

ES, also called as "electrostatic drawing", is a versatile nano- and microfabrication method, in which a high voltage is used to create an electrically charged continuous liquid jet of a polymer solution. As given jet is electrostatically drawn onto a grounded collector, the solvent evaporates or the molten polymer solidifies and the fibers are formed. Melt-electrospinning (MES) is a thermal modification of ES where instead of polymer solution a molten polymer is used as a substrate. MES has a number of advantages over a conventional solution-based ES: (1) the use of organic solvent(s) can be avoided; (2) the yield is exceptionally high (often 100%); (3) the size of fibers is uniform (diameter ± 5%), and (4) MES can be readily extended to three dimensional (3D) direct writing mode for preparing tissue engineering scaffolds (analogue of 3D printing). Despite of these significant advantages, a major limiting factor for MES is perhaps a high processing temperature, which means that only thermostable compounds can be processed (Balogh et al., 2015; Bhardwaj and Kundu, 2010). In addition, the diameter of the MES fibers is generally at a sub-micron or micron-scale instead of nano-scale (Dalton

et al., 2006; Hutmacher and Dalton, 2011). Moreover, MES can be performed with rather limited number of biocompatible water-soluble polymers in the melt (Bhardwaj and Kundu, 2010).

The most significant parameters affecting melt-electrospun fiber (MSFs) formation and diameter are feeding rate, applied voltage, temperature, polymer conductivity, polymer molecular weight, distance between the spinneret and collector, collector type and moving speed (Brown et al., 2016). The feeding rate should support the Taylor cone formation with following fiber drawing. If the rate is too slow, Taylor cone does not evolve and if too fast it might start pulsating affecting the fiber diameter. Like in conventional ES, voltage is used to draw the fiber towards collector. Voltage also stabilizes the fiber jet in case of MES. Too high voltage can lead to process instabilities (whipping). The distance between the spinneret and collector is usually in a centimetre range (Dalton et al., 2007), and it needs to be long enough to allow the fiber to solidify. However, changes in voltage might be needed to avoid the whipping. In case of specialized methods, such as near-field ES (Sun et al., 2006) and electro-hydrodynamic jet plotting (Wei and Dong, 2013), the distance between collector and the spinneret could be in a micron range. Temperature affects the process through changing polymer viscosity (higher polymer weight leads to higher viscosity). If the melt is too viscous, high processing temperatures are needed that might lead to thermal decomposition.

It is possible to reduce the MES temperature by adding plasticizers (Balogh et al., 2014). Plasticizers are usually non-volatile compounds with small molecular weight that are incorporated in a polymer matrix to lower its rigidity and improve the processing of the polymer. The addition of the plasticizer to the polymer lowers the glass transition

temperature, elastic modulus and viscosity of the melt of the mixture (Lim and Hoag, 2013). Unfortunately the lowered glass transition temperature can compromize the physical stability of the resultant SD (Craig et al., 1999). Thus, it would be preferable to use volatile plasticizers that desorb during or after processing. As the glass transition temperature of water is approximately at -135°C (Haque and Roos, 2004; Heljo et al., 2012) and it is vaporized at temperatures where MES is usually carried out, it could be a suitable candidate for a given purpose.

Temperature also affects the polymer drug miscibility during processing. There are several methods that can be used to estimate the drug polymer miscibility or the solubility of the drug in polymer at ambient conditions. Flory-Huggins theory, Gordon-Taylor equation, Hansen solubility parameter and Brostow Chiu Kalogeras Vassilikou-Dova (BCKV) equations have been used among others (Bochmann et al., 2016; Craig et al., 1999; Djuris et al., 2013; Marsac et al., 2009). Drug-polymer miscibility has also a crucial role in physical stability of the SDs. It is expected that the system would be physically stable if the drug is miscible with polymer at given conditions. For example, Bochmann et al. (2016) have calculated the solubility of our drug indomethacin (IND) in carrier polymer SOL at different temperatures using BCKV equation. They discovered that the solubility of IND is 26% (w/w) at 25°C, and that they are miscible in molten state (Bochmann et al., 2016).

To date, less than 1% of electrospinning literature is dedicated to the solvent-free approaches (Dalton, 2017). The first paper describing melt-spun filament formation from polypropylene and polyethylene was published in 1981 (Larrondo and St. John Manley, 1981). Polymers such as polycaprolactone (PCL) (Brown et al., 2011),

polyethylenglycol-polycaprolactone block polymer (PEG-b-PCL) (Dalton et al., 2008), polypropylene (PP) (Haigh et al., 2017) and poly(ethylene-co-vinyl) alcohol (EVAL) (Ogata et al., 2007) have been mostly investigated for tissue engineering rather than drug delivery purposes. The pharmaceutical applications of MES are still scarce, but in the recent years the interest towards present technique has steadily increased. Nagy et al. (2013) and Balogh et al. (2014) have successfully developed fast dissolving fibrous formulations for poorly water-soluble carvedilol using hydrophilic Eudragit® E and different plasticizers by utilizising MES and melt-blowing, respectively (Balogh et al., 2014; Nagy et al., 2013). Lian & Meng (2017) obtained modified drug release with daunorubicin-PCL loaded fibrous membranes prepared by MES (Lian and Meng, 2017).

Polyvinyl caprolactam-polyvinyl acetate-polyethylene glycol graft copolymer is a recently introduced amphiphilic polymer intended for pharmaceutical applications (BASF, 2010). It is also know as Soluplus® (SOL). SOL was originally developed as a carrier material for hot-melt extrusion (HME) and granulation processes, but due to its unique properties (thermal behaviour, solubilizing properties, binding effects, etc.), it has also been tested in other pharmaceutical manufacturing processes (Lust et al., 2013, 2015; Semjonov et al., 2017).

The primary goals of the present study were to investigate a modified MES for fabricating the MSFs intended for improving **the dissolution rate** of a poorly water-soluble drug (IND as a model drug), and to gain understanding of the physical solid-state changes, drug-carrier polymer interactions, and dissolution behaviour associated with the present MSFs. In addition, the role and effects of absorbed water on the MES process were investigated.

2. Materials and methods

2.1 Materials

Indomethacin [1-(*p*-chlorobenzoyl)-5-methoxy-2-methylindole-3-acetic acid] in a γ polymorphic form (Acros, United Kingdom) was used as a poorly water-soluble model drug. Soluplus® (SOL), polyvinyl caprolactam-polyvinyl acetate polyethylene glycol graft copolymer (BASF SE Pharma Ingredients & Services, Ludwigshafen, Germany) was used as a carrier polymer.

2.2 Methods

2.2.1 Preparation of physical mixtures (PMs)

Raw materials were passed through a 150-μm size sieve. The physical mixtures (PMs) were prepared by mixing SOL with IND in mortar with pestle as described in our previous paper (Semjonov et al., 2017). The batch size of each PM was 6.0 g. The PM1 consisted of crystalline γ-IND and SOL (1:3). The PM2 consisted of amorphous IND prepared by quench cooling of a melt and SOL at a 1:3 weight ratio. The PM3 was obtained storing a PM1 on a Petri dish at high relative humidity (~90%) for 72 hours. The PMs 1 and 2 were used as the reference samples and PM3 was used in the MES experiments for MSF preparation.

2.2.2 Melt electrospinning (MES)

Prior to MES, the PM3 was stored at 90% RH and at an ambient room temperature for 72 hours. The MSFs were prepared with an ESR200RD system (NanoNC Co. Ltd., Seoul, Republic of Korea) equipped with a special MES spinneret (metal syringe with attached needle) coupled with a thermostated oil bath circulator (NanoNC Co. Ltd., Seoul, Republic of Korea) (Fig. 1). The MES of drug-loaded fibers was performed at 180 °C and at a voltage of 5-10 kV (Model HV30 high-voltage power supply unit). The angle of spinneret was set at 25°, and the distance between a spinneret and fiber collector was 5.0 cm. The collector was grounded. The process was driven by build-in pressure from water evaporation, hence without the need for applied feeding rate. Fibers were colleted on a rotating drum (15 rpm). The MSFs of pure carrier polymer (SOL) was used as a reference to drug-loaded fibers. Prepared MSFs were stored in a desiccator at 15% RH (23 °C). MSFs were further processed by grinding them in mortar with pestle. The obtained powder was used for analysis and dissolution testing.

Figure 1. Schematic illustration of a melt electrospinning (MES) device with a heating system based on oil circulating through the jacket placed around the metal syringe. Arrow points out circulating heated oil and the direction of the collector movement. The symbol P designates build-in pressure from water evaporation.

2.2.3 Thermal analysis

A DSC 4000 differential scanning calorimeter (Perkin Elmer Ltd., Shelton, CT, USA) was used for the thermal analysis of MSF samples in an aluminum pans with pinholes in

a lid and under a dry nitrogen flow. The samples (2-8 mg) were heated from 20 to 200 °C at a rate of 10 °C/min. The DSC system was calibrated with indium.

Thermogravimetric analysis (TGA) was performed with a NETZSCH STA 449 F3 Jupiter®, (NETZSCH- Gerätebau GmbH, Germany) simultaneous thermal analyzer in order to study a mass loss and thermal degradation of the samples upon heating. Oxygen nitrogen mixture (in the ratio of 20 to 80) was used as a purge gas at the flow rate of 60 ml/min. Samples (25-35 mg) were placed on a corundum sample holders. The sample was heated from 20 °C to 350 °C at the rate of 10 °C/min and held isothermally at 350 °C for 10 min. Data were processed with NETZSCH Proteus® Software for Thermal Analysis. Temperatures are given as onset-points unless otherwise mentioned.

2.2.4 High-Performance Liquid Chromatography (HPLC)

The total amount and chemical stability of IND in MSF (three different batches, n=8) was determined by means of HPLC (254 nm) using slightly modified European Pharmacopoeia (Eur. Ph) method for IND. HPLC system (Shimadzu Prominence LC20 with PDA detector SPD-M20A) controlled by software LCsolution was used. Standard of IND (~0.15 mg/mL) was dissolved in acetonitrile:water solution (1:1). The column Phenomenex Luna2 C18 was used with the flow rate of 1.0 mL/min and injection volume of 10 µL at the temperature of 50 °C. Following mobile phases were used: (A) a 0.3% (m/V) solution of acetic acid in water, (B) a solution containing **0.3**% (m/V) acetic acid and 0.7% (m/V) of water in acetonitrile. Retention time of IND was about 8 min. HPLC was also used to confirm the results of drug release from MSF obtained by UV-Vis spectrophotometer.

2.2.5 Scanning electron microscopy (SEM)

A high-resolution scanning electron microscope (SEM) (Zeiss EVO MA 15, Carl Zeiss Microscopy GmBH, Germany) was used for imaging the surface morphology and diameter of MSFs. The samples were imaged without coating in argon atmosphere under high pressure at different magnifications. Furthermore, the surface morphology and porosity (internal voids within fibers and voids/pores on the fiber surface) were analysed using SEM micrographs and ImageJ software was used for calculating the pore size.

2.2.6 X-ray powder diffraction (XRPD)

The XRPD patterns of rotating samples were collected using Bruker D8 Advance diffractometer (Bruker AXS GmbH, Germany) using Cu Kα1 radiation (λ=1.5418 Å, 40 kV and 40 mA). Data were gathered in theta–theta geometry in the range of 5°–35° 2θ, (with the step size of 0.0195° 2θ) and with a LynxEye positive sensitive detector.

2.2.7 Fourier transform infrared spectroscopy (FTIR)

Fourier transform infrared spectroscopy (FTIR) of samples was performed with IR Prestige-21 Spectrophotometer (Schimadzu Corp., Kyoto, Japan) and Specac Golden Gate Single Reflection ATR crystal (Specac Ltd., Orpington, UK). Operating range was 4000–600 cm^{-1}. The final spectrum was the mean of 60 scans and each sample was measured in triplicate.

2.2.8 Nuclear magnetic resonance (NMR) spectroscopy

^{1}H and ^{13}C FT-NMR-spectra in $CDCl_3$ (Eur-isotop 99.80% containing 0.03% TMS) solution together with ^{13}C CP-MAS spectra in solid state were recorded using Bruker Avance III 500 MHz spectrometer (Bruker, UK Limited, United Kingdom). ^{13}C-CP-MAS-spectra were recorded for the pure materials as well as for PM1 and MSFs using 10 kHz rotation, 3 ms contact time and 10 s delay between pulses. The ^{1}H-spectra of IND and SOL together with their PM1 and MSFs were recorded with the materials dissolved in deuterochloroform. Solution spectra were recorded in 5 mm glass tubes and solid state spectra in 4 mm rotors. All spectra were recorded at 23 °C.

2.2.9 Dissolution test

The dissolution tests were carried out in a Distek Dissolution system 2100B (Distek, Inc., North Brunswick, New Jersey, USA). The United States Pharmacopeia (USP) paddle method (Type 2) was used for dissolution testing. The samples (n = 3) were analyzed using an UV-Vis spectrophotometer (Specord® 200 Plus, Analytik Jena AG, Germany) at 370 nm. It was confirmed that neither SOL nor MSFs from pure SOL showed any absorption at 370 nm. The samples were manually withdrawn at fixed time intervals (10 min, 20 min, 30 min, 60 min, 120 min) and filtered (0.45 µm membrane) before analysis. Degasified buffer solution (pH = 6.8) with a total volume of 500 ml at 37.0 ± 0.5 °C was used as a dissolution medium. The paddle rotation speed was set at 100 rpm. All tests were perfomed in triplicate.

2.2.10 Data analysis

The fiber size of MSFs (n=30-50) was measured with ImageJ (version. 1.50i). Data are expressed as a mean ± SD. Statistical analysis was performed with a 2-tailed unpaired t-test using MS Excel Software 2010. The level of significance was set at $p < 0.05$ (denoted on the figures by *). Origin Pro 8.5 (Origin Lab Corporation) was used to draw the figures.

3. Results and discussion

3.1 Design and fabrication of melt-electrospun fibers

MES is a continuous bottom-up technique for preparing polymeric fibrous systems at a nano- or micro-scale. MES does not use any organic solvents, and consequently, no subsequent drying phase is needed. We determined the critical MES parameters necessary for the fabrication of the MSFs of the present drug (IND) and carrier polymer (SOL) (i.e., temperature, voltage, distance between a melt spinneret and collector, and the angle of spinneret, speed of rotating collector). The feeding rate was calculated from the time taken for the sample to be electrospun. As it took approximately 30 minutes to spin the 6 gram sample, the feeding rate was 12 g/h.

At first, PM1 was electrospun directly without pre-storing it at high RH. Due to high viscocity of the melt, it was necessary to increase the temperature of the process to 220 °C and specific smell and colour changes indicated the degradation of the drug. Pre-storing the samples at high humidity (above 90% RH) in dessiccator prior MES experiments was used in order to plasticize the PM1. The water sorption in the PM samples was verified by collecting the NIR spectra from the samples stored at different humidities (Appendix) and measuring TGA (s.f. paragraph 3.2 “Thermal analysis”). Pre-storing the samples at high humidity enabled to lower the processing temperature of MES by 40 °C (to 180 °C). Hence, the addition of plasticizer (in our case water) was of critical importance. In addition, water vapor heated up to 180°C created additional pressure that probably helped to overcome the high viscosity of the polymer melt.

3.2 **Thermal analysis**

Similarly to widely used hot-melt extrusion (HME) also in MES the materials are subjected to a short-term high temperature and pressure during the process. These conditions can cause the chemical degradation of drug, polymer or both. According to the literature, the thermal decomposition of IND is a one-step phenomenon within the temperature range of 236-338 °C (Tita et al., 2009a). The IND has a good safety margin for thermal processing at lower temperatures. According to Forster et al. (2001), the chemical stability of IND in PVP/IND dispersions at different weight ratios (1:1 and 4:1) after HME at 170 °C was good, since only less than 1% of drug was decomposed. Melt extrusion of acrylic polymers/IND (30% drug concentration) showed that IND is chemically stable after exposure to high temperature (140 °C) (Zhu et al., 2006). SOL is thermally stable up to 220°C showing no changes in chemical composition or degree of polymerization (BASF, 2010; Kolter et al., 2012).

The results of thermogravimetric analysis (TGA) of pure materials and PMs are depicted in **Fig. 2A**. Weight loss of the samples up to 150 °C was assigned to water evaporation upon heating. Given values were used to estimate the amount of water absorbed by SOL and PMs. The SOL contained 2.4% and the PM1 contained 1.6% of water by weight. After storage at high relative humidity (90%) the PM3 contained 7.4% of water by weight. IND was found to be a thermally stable compound at the temperature that was used for MES (only 0.1% of weight loss at 180 °C was detected). The thermal degradation of IND and SOL started at 197.1 °C and 218.2 °C, respectively. According to the literature, the thermal degradation of IND occurs approximately at 236 to 338 °C

(with T_{max} 314 °C) (Tita et al., 2009b). The present results are in agreement with those reported in the literature, where a 2.5% weight loss of SOL was detected at low temperatures, and the degradation of the material started approximately at 250 °C (Kolter et al., 2012). In summary, TGA results suggest that MES performed at 180 °C is a non-destructive process and does not cause (or causes only minimal) thermal degradation for the present materials. A long-term exposition of materials to MES process, however, will most likely result in thermal degradation of the materials.

The TGA results were in line with the DSC results, where γ-IND showed a sharp melting endotherm at 161.8 °C (without any water desorption), and SOL showed a broad water evaporation endotherm until 76.3 °C (indicating also a substantial amount of water in the samples) (**Fig. 2B)**. The DSC thermographs of PM1 showed a broad water evaporation endotherm derived from SOL within PMs and a broad fusion endotherm of γ-IND into SOL starting at 115.7 °C. The fusion endotherm ended with a minor sharp endotherm at 160.1 °C, which was attributed to the melting of residual γ-IND. The PM2, containing amorphous IND and SOL at the weight ratio 1:3 (drug:polymer) presented the Tg of IND at 50.6 °C and a water evaporation endotherm. In addition, a small exothermic peak was recorded for PM2 at 83.8 °C, and it was assigned to the crystallization of IND. The onset temperature of the subsequent fusion endotherm for recrystallized IND was recorded at 107.0 °C. The PM3 (stored at high RH 90%) thermogram mirrored the results of PM1. As expected, the thermal behavior of PMs revealed the behavior of the pure materials alone **(Fig. 2B)**. The DSC thermograph of MSF indicates the formation of amorphous SD, since no signs of recrystallization and melting endotherm of IND were detected, which might indicate at least partial mixing of a drug in a molten polymer (**Fig. 2B**).

Figure 2. Thermogravimetric analysis (TGA) (A) and differential scanning calorimetry (DSC) thermograms (B) of starting materials, physical mixtures (PMs) and melt-electrospun fibers (MSF). Key: γ-IND – indomethacin, SOL - Soluplus®, PM1 – the physical mixture of crystalline γ-IND and SOL at the weight ratio 1:3 (drug:polymer), PM2 – the physical mixture of amorphous IND and SOL at the weight ratio 1:3 (drug:polymer), PM3 – the PM1 stored at high RH (90%), MSF – melt-electrospun fibers prepared from PM3. The actual process temperature of MES (180 °C) is indicated with a solid line in the figure.

3.3 **Indomethacin content assessment within MSFs**

In our study, the total drug content of MSFs was assayed/verified by HPLC. Three different MES batches were analysed in duplicate or triplicate (theoretical drug content was 25%). The following drug contentents for different MSF batches were measured: 23.2 ± 0.15% (n=3) for batch 1; 23.8 ± 0.6% (n=3) for batch 2; and 23.5 ± 0.4% (n=2) for batch 3. These values are in close proximity to the theoretical drug content values confirming that the present MES process is stable and reproducible resulting in small drug content variation. Given results are in a good agreement with the data presented in literature. It is known that IND (Tita et al., 2009a) and SOL (Kolter et al., 2012) are both stable at the conditions they were presented during the MES.

3.4 **Fiber size, shape and surface morphology**

The fiber size and morphology of drug-loaded MSFs (IND and SOL at the weight ratio of 1:3) and the corresponding blank MSFs are presented in **Fig. 3**. The diameter of drug loaded MSFs varied from 300 to 400 µm and the diameter of blank MSFs ranged from 200 µm to 400 µm. As reported elsewhere, the diameter of MSF can vary even from 270 nm (i.e., nano-scale) to 500 µm (micro-scale) (Dalton et al., 2006; Lyons et al., 2004). Such a wide size range option in fiber diameters shows the flexibility of MES. In our study, the large micro-scale size of MSFs could be explained by high molecular weight of SOL (90 000 – 140 000 g/mol) (BASF, 2010). According to the literature, the molecular weight of a thermal carrier polymer is a critical factor determining the final fiber diameter in MES (Lyons et al., 2004).

The surface morphology of the present MSFs (**Fig. 3A**) was smooth without any voids or pores, but clearly shrunken and billowy for the whole fiber area. This could be explained by a thermal shock induced by the temperature difference during MES when the fibers are produced and collected. The shrinking was more pronounced with blank MSFs (**Fig. 3B**), thus showing a higher polymer chain mobility compared to the drug loaded MSF. It is well known that higher surface area results in higher dissolution rate (Noyes and Whitney, 1897). Hence the major advantage of shrunken and billowy MSFs compared to the smooth fibers is larger specific surface area, and thus their dissolution rate should be faster compared to the smooth surfaced fibers/particles. **Also, the supersaturation ratio has been shown to be an important factor governing the passive transportation of poorly-water soluble drugs from supersaturated solutions (Borbás et al., 2016)**

Figure 3. The SEM images of (A1) intact melt-electrospun fibers (MSF) of γ-IND and SOL at the weight ratio of 1:3 (drug to polymer), (A2) the corresponding ground MSFs, (B1) blank MSFs, and (B2) the corresponding ground blank MSFs. Key: γ-IND – indomethacin, SOL – Soluplus®.

The SEM image of the drug loaded MSFs cross-section (**Fig. 3A1**) shows a non-uniform structure of the fiber. At some places, the fibers are hollow and at others they do not have any inner voids at all. The cross section of blank fiber (as shown in **Fig. 3B1**) consisted of primarily intact solid surface with very small voids. The difference in the morphology of drug-loaded and blank MSFs could be related to the different molecular mobility and rigidity of the IND containing SOL and pure SOL during MES process. As mentioned earlier, the instability of a MES process could also partially explain the formation of MSFs with such a complicated structure. **Fig. 3** shows also the SEM images of drug-loaded (**A2**) and blank (**B2**) MSFs in a powder form after grinding. The partially hollow structure of the original MSFs can still be seen even after grinding (**Fig. 3A2**). These cavities are evidently the former water vapor channels inside a fiber matrix, and they are formed as water evaporates from the matrix or extrudate during fiber formation (Miladinov and Hanna, 1999).

SEM micrographs together with ImageJ software was used for calculating the size of the resultant water vapor channels in our materials. The average pore size for the intact drug-loaded and blank MSFs were 28.2 μm (ranging from 0.5 to 301.4 μm) and 13.3 μm

(ranging from 3.0 to 59.6 μm), respectively. The average pore size for the ground drug-loaded and ground blank MSF particles was 32.5 μm (ranging from 8.4 to 65 μm) and 40.8 μm (ranging from 2.4 to 109 μm), respectively. The average pore sizes for the drug-loaded MSFs and ground drug loaded MSF powder were quite similar but the variation (range) was great. The difference in variability is obviously due to a grinding process that breaks up the delicate tube structure of the drug-loaded MSFs resulting in plate like particles (**Fig. 3A2**). The difference in the pore size of the intact blank MSFs and the respective powder sample can be explained by opening of the closed and bottle-like pores due to grinding.

Sorbed water can act as (1) a direct reactant (hydrolytic reactions), (2) a chemical reactivity inhibitor (Maillard reaction), (3) a solvent system, and (4) an external plasticizer (Shalaev and Zografi, 1996). In our system, water acted as a plasticizer, thus reducing the viscosity of the melt and improved the performance of a MES. The plasticizing effect of water has been previously shown for starches prior extrusion into the foams (Shogren, 1996; Sjöqvist and Gatenholm, 2005). In the case of starch extrusion, water added in the system is entrapped inside the cavities of the extrudate, and after leaving extruder, it evaporates and forms channels in the matrix (Miladinov and Hanna, 1999). It is evident that similar interaction with water also occurs in the present MES process, thus resulting in the formation of partially hollow MSF structures.

3.5 **Physical solid state and drug-carrier interactions**

The XRPD was used to detect the potential physical solid-state changes of the components in a MES process. As shown in **Fig. 4**, the drug (IND) in the PM1 preserved

its γ-IND crystalline form after mixing with SOL (a slightly elevated baseline of amorphous SOL can be also seen). As expected, the PM of amorphous IND and SOL (PM2) showed only an amorphous halo. In case of PM3 (the PM was stored at RH 90%), the XRPD pattern showed minor intensity changes, but the γ-IND reflections were clearly distinguishable. The polymorphic transformation of an amorphous IND to α-IND at such a high RH reported in literature (Savolainen et al., 2007) was not detected in this study. Evidently the addition of polymer (SOL) can significantly alter the crystallization behavior of an amorphous material. The MSFs of IND and SOL (originated from the PM3) showed the XRPD pattern with a clear amorphous halo, thus confirming the formation of an amorphous SD (**Fig. 4**).

Figure 4. X-ray powder diffraction (XRPD) patterns of starting materials, physical mixtures (PMs) and melt-electrospun fibers (MSF). Key: γ-IND – indomethacin, SOL – Soluplus®, PM1 – the physical mixture of crystalline γ-IND and SOL at the weight ratio 1:3 (drug:polymer), PM2 – the physical mixture of amorphous IND and SOL at the weight ratio 1:3 (drug:polymer), PM3 – the PM1 stored at high RH (90%), MSF – melt-electrospun fibers prepared from PM3. All patterns are normalized and off-set for clarity.

FTIR spectroscopy was used to investigate the potential drug-carrier polymer interactions during MES. In our study, a special attention was paid to the region between 1650 and 1750 cm^{-1} which is characteristic to IND carbonyl (C=O) stretching bands (Ewing et al., 2014). As seen in **Fig. 5**, the FTIR spectrum of γ-IND contains two bands in this region. The peaks at 1688 cm^{-1} and 1711 cm^{-1} were assigned to the benzoyl C=O

and assymetric stretch of the carbocylic acid bands, respectively. The present results are in accordance with the wavenumbers reported for C=O bands in the literature (Ewing et al., 2014; Lin et al., 2015; Terife et al., 2012). The spectra of PM1 and PM3 are quite similar. Both contain the benzoyl C=O vibration band at 1688 cm^{-1}. Due to spectral overlapping with the SOL ester C=O band at 1732 cm^{-1}, the band assigned to the assymetric stretch of the carbocylic acid is located at 1715 cm^{-1} in the spectra of PM1 and PM3. The benzoyl C=O vibration band appears at 1682 cm^{-1} in the spectra of MSFs and PM2. According to the literature, the band at this wavenumber is specific to amorphous IND (Ewing et al., 2014; Lin et al., 2015; Terife et al., 2012). The spectrum of PM2 contains a shoulder to the SOL ester C=O band at 1709 cm^{-1} that has been assigned to hydrogen bonded carbocylic acid C=O in amorphous IND molecules arranged as chains or dimers in the literature (Ewing et al., 2014; Lin et al., 2015; Terife et al., 2012). This feature is lacking in the spectrum of MSFs. This difference in the spectra could indicate at least partial hydrogen bonding between IND and SOL molecules in MSFs.

Figure 5. Fourier Transform Infrared (FTIR) spectra of starting materials, physical mixtures (PMs) and melt-electrospun fibers (MSF) Key: γ-IND – indomethacin, SOL – Soluplus®, PM1 – the physical mixture of crystalline γ-IND and SOL at the weight ratio 1:3 (drug:polymer), PM2 – the physical mixture of amorphous IND and SOL at the weight ratio 1:3 (drug:polymer), PM3 – the PM1 stored at high RH (90%), MSF – melt-electrospun fibers prepared from PM3. All patterns are normalized and off-set for clarity.

3.6 ^{1}H and ^{13}C FT-NMR spectroscopy

^{1}H-spectra of PM1 and MSFs were recorded after dissolving the materials in deuterochloroform. The chemical shifts of the IND and SOL coincided for the two mixtures and no signs of thermal degradation were observed for the electrospun mixture **(Fig. 6A)**.

Figure 6. Overlay of 1H-spectrum of physical mixture (PM) and melt-electrospun fibers (MSFs) (A) and ^{13}C CP-MAS-spectra of starting materials, physical mixtures (PMs) and melt-electrospun fibers (MSF) (B). Key: γ-IND – indomethacin, SOL – Soluplus®, PM1 – the physical mixture of crystalline γ-IND and SOL at the weight ratio 1:3 (drug:polymer), MSF – melt-electrospun fibers prepared from PM3 (the PM1 stored at high RH (90%).

^{13}C FT-NMR spectroscopy (^{13}C CP-MAS-spectra) results are shown in **Fig. 6B.** ^{13}C-CP-MAS-spectrum of the PM1 shows the chemical shifts of both substances as a direct superposition of the spectra of the pure materials. In the PM1, IND is still in the γ-form as indicated by the lack of splitting of the signals as reported previously (Masuda et al., 2006). For the MSFs, the chemical shifts show a marked change as in general the signals from γ-IND are broadened significantly and nearby signals are merged together. As the signals from the pure SOL are already quite broad, similar changes were not observed for SOL in MSFs. This change in the IND spectra can be considered as an indication of more intimate mixing of the substances during a MES process.

In order to get more information about the difference of IND in the PM1 and MSFs, the T1(^{1}H) was recorded for solid state samples using the inversion recovery technique and

the relaxation delay was varied from 0.500 to 200 s. For mixtures with small domain sizes spin diffusion results in just one T1(^{1}H), i.e. magnetization in the regions that would otherwise have longer T1(^{1}H) diffuses into regions with shorter T1(^{1}H). It has been shown in a previous study (Brettmann et al., 2012), that equation 1 can be used to calculate the approximate domain sizes.

$$L = (6DT_i)^{1/2} \qquad \text{Eq. 1}$$

In the Eq. 1, L is the magnetization diffusion length, D is the spin diffusion coefficient and T_i is the relaxation time. In this study, approximate values of D, 8.0×10^{-16} m^2/s for rigid systems and 0.5×10^{-16} m^2/s for mobile systems were used, which were reported earlier by Spiegel et al. (1994). Because the rigidity/flexibility of the system is not precisely known we present the domain sizes as a range and the result gives upper limits for the domain size. To avoid the possible overlapping of the signals, inversion recovery of only two regions were followed. Signals in the approximate region of 63-76 ppm originate exclusively from SOL and 125-138 ppm from IND. The measured T1(^{1}H) of SOL (63-76 ppm) is 2.061 s for the PM1 and 2.067 s for the MSFs, and they can be considered to be practically the same. However, the measured T1(^{1}H) of IND (125-138 ppm) in the PM1 is 4.524 s compared to that of 2.165 s for the MSFs. This gives IND a domain size range of 25-100 nm for the MSFs. The very similar values of T1(^{1}H) for both IND and SOL in the MSFs can be considered as a strong indication of significantly smaller domain size of the IND in the SOL matrix compared to the PM1. The T1ρ^{1}H, which would give information about the domain size within the range of 2-20 nm, were not measured as the long spin-lock times would have seriously damaged the probe.

3.7 Dissolution

In our study, the powder samples prepared form intact MSFs were subjected to *in-vitro* drug release studies. The dissolution rate of MSFs and PM2 (amorphous IND) was significantly higher than that of crystalline γ-IND powder (**Fig. 7**). The PM1 showed the slowest drug release, probably due to the gel formation of the polymer (SOL). Such observation is consistent with the previous findings (Terife et al., 2012). Almost complete drug release from MSFs was observed within 30 min (88.7±0.5%), while the amount of drug released from the corresponding PM1 and PM2 at the same time point of the experiment was only 16.1±1.1% and 38.1±5.7%, respectively. It is well-known that amorphous IND has nearly 1.4 fold higher solubility in water compared to its crystalline form (Imaizumi et al., 1980; Hancock and Parks, 2000). The improved release rate of IND from MSFs is evidently due to amorphous state and smaller domain size of IND compared to PM1 and PM2. Furthermore, MSFs in a powder form provide a higher effective surface area compared to other solid state forms. This is due to a specific morphology of the powder particles obtained by grinding the present MSFs (i.e., partially plate shaped particles). These properties have been reported to have an significant effect on the release rate of a poorly water-soluble drugs (Hancock and Parks, 2000; Hughey et al., 2013; Merisko-Liversidge and Liversidge, 2011). Our results are also in accordance with those reported by Balogh et al. (2014) and Nagy et al. (2013), who found that the drug release from MSF was comparable to the fibers fabricated by solvent-based electrospinning (SES) and superior to PMs and drug alone (Balogh et al., 2014; Nagy et al., 2013).

Figure 7. *In vitro* dissolution profiles of γ-IND, physical mixtures (PMs) and melt-electrospun fibers (MSF) at the weight ratio 1:3 (drug:polymer) in pH 6.8 phosphate buffer (n=3). Key: γ-IND – indomethacin, PM1 – the physical mixture of crystalline γ-IND and SOL at the weight ratio 1:3 (drug:polymer), PM2 – the physical mixture of amorphous IND and SOL at the weight ratio 1:3 (drug:polymer), MSF – melt-electrospun fibers prepared from PM3. The error bars indicate the standard deviations (n = 3).

4. Conclusions

We showed that MES is an auspicious novel method for fabricating amorphous SDs for poorly water-soluble drugs. The use of water in a controlled manner enabled to lower the MES temperature significantly through a plasticization effect and by creating additional pressure in a syringe. Only minimal thermal degradation of a model drug (IND) is associated with the fabrication of MSFs in a MES process. Solid-state analysis suggests more intimate mixing between IND and an amorphous stabilizing carrier material (SOL) in the present MSFs. The MSFs of IND and SOL provided significantly faster drug dissolution (within 30 min) compared to the corresponding PMs and crystalline drug. In summary, (1) the diameter of the present MSFs is at a micron scale; (2) the IND is rendered amorphous in MSF; (3) MSFs have a high surface area; (4) water as a plasticizer can reduce the temperature of MES process; (5) both SOL and IND remain chemically stable during a MES process, and (6) the dissolution of a drug (IND) is rapid from MSFs. Therefore, the MSFs produced by MES could be an alternative strategy in improving **the dissolution rate**, and consequently the oral bioavailability of poorly water-soluble drugs.

Conflict of interest

The authors declare no conflicts of interest.

Acknowledgements

The work is part of the Estonian national research projects (PUT1088 and IUT-34-18). Estonian Research Council and the Ministry of Education and Research are acknowledged for funding. Prof. K. Kirsimäe, MSc. J. Aruväli and MSc. M. Külaviir (The X-ray laboratory, Department of Geology, Institute of Ecology and Earth Sciences, University of Tartu, Estonia) are acknowledged for performing the SEM and XRPD experiments. Undergraduate students A. Ringe from the University of Tartu and F. Lompart from the Pavol Jozef Šafárik University in Košice are thanked for conducting part of the MES and dissolution experiments.

References

Balogh, A., Drávavölgyi, G., Faragó, K., Farkas, A., Vigh, T., Sóti, P.L., Wagner, I., Madarász, J., Pataki, H., Marosi, G., Nagy, Z.K., 2014. Plasticized Drug-Loaded Melt Electrospun Polymer Mats: Characterization, Thermal Degradation, and Release Kinetics. J. Pharm. Sci. 103, 1278–1287. https://doi.org/10.1002/jps.23904

Balogh, A., Farkas, B., Faragó, K., Farkas, A., Wagner, I., Van Assche, I., Verreck, G., Nagy, Z.K., Marosi, G., 2015. Melt-blown and electrospun drug-loaded polymer fiber mats for dissolution enhancement: A comparative study. J. Pharm. Sci. 104, 1767–1776. https://doi.org/10.1002/jps.24399

BASF, 2010, 2010. BASF. Safety Data Sheet, Soluplus®. BASF, Pharma Ingredients Serv. 1–7.

Bhardwaj, N., Kundu, S.C., 2010. Electrospinning: A fascinating fiber fabrication technique. Biotechnol. Adv. 28, 325–347. https://doi.org/10.1016/j.biotechadv.2010.01.004

Bochmann, E.S., Neumann, D., Gryczke, A., Wagner, K.G., 2016. Micro-scale prediction method for API-solubility in polymeric matrices and process model for forming amorphous solid dispersion by hot-melt extrusion. Eur. J. Pharm. Biopharm. 107, 40–48. https://doi.org/10.1016/j.ejpb.2016.06.015

Borbás, E., Sinkó, B., Tsinman, O., Tsinman, K., Kiserdei, É., Démuth, B., Balogh, A., Bodák, B., Domokos, A., Dargó, G., Balogh, G.T., Nagy, Z.K., 2016. Investigation and Mathematical Description of the Real Driving Force of Passive Transport of Drug Molecules from Supersaturated Solutions. Mol. Pharm. 13, 3816–3826. https://doi.org/10.1021/acs.molpharmaceut.6b00613

Brettmann, B., Bell, E., Myerson, A., Trout, B., 2012. Solid-State NMR

Characterization of High-Loading Solid Solutions of API and Excipients Formed by Electrospinning. J. Pharm. Sci. 101, 1538–1545. https://doi.org/10.1002/jps.23032

Brown, T.D., Dalton, P.D., Hutmacher, D.W., 2016. Melt electrospinning today : An opportune time for an emerging polymer process. Prog. Polym. Sci. 56, 116–166. https://doi.org/10.1016/j.progpolymsci.2016.01.001

Brown, T.D., Dalton, P.D., Hutmacher, D.W., 2011. Direct Writing By Way of Melt Electrospinning. Adv. Mater. 23, 5651–5657. https://doi.org/10.1002/adma.201103482

Craig, D.Q.M., Royall, P.G., Kett, V.L., Hopton, M.L., 1999. The relevance of the amorphous state to pharmaceutical dosage forms: Glassy drugs and freeze dried systems. Int. J. Pharm. 179, 179–207. https://doi.org/10.1016/S0378-5173(98)00338-X

Dalton, P.D., 2017. Melt electrowriting with additive manufacturing principles. Curr. Opin. Biomed. Eng. 2, 49–57. https://doi.org/https://doi.org/10.1016/j.cobme.2017.05.007

Dalton, P.D., Grafahrend, D., Klinkhammer, K., Klee, D., Möller, M., 2007. Electrospinning of polymer melts: Phenomenological observations. Polymer (Guildf). 48, 6823–6833. https://doi.org/10.1016/J.POLYMER.2007.09.037

Dalton, P.D., Joergensen, N.T., Groll, J., Moeller, M., 2008. Patterned melt electrospun substrates for tissue engineering. Biomed. Mater. 3. https://doi.org/10.1088/1748-6041/3/3/034109

Dalton, P.D., Lleixà Calvet, J., Mourran, A., Klee, D., Möller, M., 2006. Melt electrospinning of poly-(ethylene glycol-block-ε-caprolactone). Biotechnol. J. 1, 998–1006. https://doi.org/10.1002/biot.200600064

Di, L., Kerns, E.H., Carter, G.T., 2009. Drug-like property concepts in pharmaceutical design. Curr. Pharm. Des. 15, 2184–2194. https://doi.org/10.2174/138161209788682479

Djuris, J., Nikolakakis, I., Ibric, S., Djuric, Z., Kachrimanis, K., 2013. Preparation of carbamazepine–Soluplus® solid dispersions by hot-melt extrusion, and prediction of drug–polymer miscibility by thermodynamic model fitting. Eur. J. Pharm. Biopharm. 84, 228–237. https://doi.org/10.1016/j.ejpb.2012.12.018

Ewing, A. V, Clarke, G.S., Kazarian, S.G., 2014. Stability of indomethacin with relevance to the release from amorphous solid dispersions studied with ATR-FTIR spectroscopic imaging. Eur. J. Pharm. Sci. 60, 64–71. https://doi.org/10.1016/j.ejps.2014.05.001

Forster, A., Hempenstall, J., Tucker, I., Rades, T., 2001. Selection of excipients for melt extrusion with two poorly water-soluble drugs by solubility parameter calculation and thermal analysis. Int. J. Pharm. 226, 147–161. https://doi.org/https://doi.org/10.1016/S0378-5173(01)00801-8

Haigh, J.N., Dargaville, T.R., Dalton, P.D., 2017. Additive manufacturing with polypropylene microfibers. Mater. Sci. Eng. C 77, 883–887. https://doi.org/https://doi.org/10.1016/j.msec.2017.03.286

Hancock, B.C., Parks, M., 2000. What is the true solubility advantage for amorphous pharmaceuticals? Pharm. Res. 17, 397–404.

Haque, M.K., Roos, Y.H., 2004. Water Plasticization and Crystallization of Lactose in Spray-dried Lactose/Protein Mixtures. J. Food Sci. 69, FEP23-FEP29. https://doi.org/10.1111/j.1365-2621.2004.tb17863.x

Heljo, V.P., Nordberg, A., Tenho, M., Virtanen, T., Jouppila, K., Salonen, J., Maunu, S.L., Juppo, A.M., 2012. The effect of water plasticization on the molecular

mobility and crystallization tendency of amorphous disaccharides. Pharm. Res. 29, 2684–2697. https://doi.org/10.1007/s11095-011-0658-4

Hughey, J.R., Keen, J.M., Miller, D.A., Kolter, K., Langley, N., McGinity, J.W., 2013. The use of inorganic salts to improve the dissolution characteristics of tablets containing Soluplus®-based solid dispersions. Eur. J. Pharm. Sci. 48, 758–766. https://doi.org/10.1016/j.ejps.2013.01.004

Hutmacher, D.W., Dalton, P.D., 2011. Melt electrospinning. Chem. - An Asian J. 6, 44–56. https://doi.org/10.1002/asia.201000436

Imaizumi, H., Nambu, N., Nagai, T., 1980. Stability and Several Physical Properties of Amorphous and Crystalline Forms of Indomethacin. Pharm. Soc. Japan 28, 2565–2569. https://doi.org/10.1248/cpb.28.2565

Kolter, E., Karl, M., Gryczke, A., 2012. Hot-Melt Extrusion with BASF Pharma Polymers.

Larrondo, L., St. John Manley, R., 1981. Electrostatic fiber spinning from polymer melts. I. Experimental observations on fiber formation and properties. J. Polym. Sci. Polym. Phys. Ed. 19, 909–920. https://doi.org/10.1002/pol.1981.180190601

Lian, H., Meng, Z., 2017. Melt electrospinning of daunorubicin hydrochloride-loaded poly (ε-caprolactone) fibrous membrane for tumor therapy. Bioact. Mater. 2, 96–100. https://doi.org/https://doi.org/10.1016/j.bioactmat.2017.03.003

Lim, H., Hoag, S.W., 2013. Plasticizer Effects on Physical–Mechanical Properties of Solvent Cast Soluplus® Films. AAPS PharmSciTech 14, 903–910. https://doi.org/10.1208/s12249-013-9971-z

Lin, S.-Y., Lin, H.-L., Chi, Y.-T., Huang, Y.-T., Kao, C.-Y., Hsieh, W.-H., 2015. Thermoanalytical and Fourier transform infrared spectral curve-fitting techniques used to investigate the amorphous indomethacin formation and its physical

stability in Indomethacin-Soluplus® solid dispersions. Int. J. Pharm. 496, 457–465. https://doi.org/10.1016/j.ijpharm.2015.10.042

Lust, A., Laidmäe, I., Palo, M., Meos, A., Aaltonen, J., Veski, P., Heinämäki, J., Kogermann, K., 2013. Solid-state dependent dissolution and oral bioavailability of piroxicam in rats. Eur. J. Pharm. Sci. 48, 47–54. https://doi.org/https://doi.org/10.1016/j.ejps.2012.10.005

Lust, A., Strachan, C.J., Veski, P., Aaltonen, J., Heinämäki, J., Yliruusi, J., Kogermann, K., 2015. Amorphous solid dispersions of piroxicam and Soluplus®: Qualitative and quantitative analysis of piroxicam recrystallization during storage. Int. J. Pharm. 486, 306–314. https://doi.org/10.1016/j.ijpharm.2015.03.079

Lyons, J., Li, C., Ko, F., 2004. Melt-electrospinning part I: processing parameters and geometric properties. Polymer (Guildf). 45, 7597–7603. https://doi.org/10.1016/j.polymer.2004.08.071

Marsac, P.J., Li, T., Taylor, L.S., 2009. Estimation of Drug – Polymer Miscibility and Solubility in Amorphous Solid Dispersions Using Experimentally Determined Interaction Parameters 26, 40–44. https://doi.org/10.1007/s11095-008-9721-1

Masuda, K., Tabata, S., Kono, H., Sakata, Y., Hayase, T., Yonemochi, E., Terada, K., 2006. Solid-state 13C NMR study of indomethacin polymorphism. Int. J. Pharm. 318, 146–153. https://doi.org/10.1016/j.ijpharm.2006.03.029

Merisko-Liversidge, E., Liversidge, G.G., 2011. Nanosizing for oral and parenteral drug delivery: A perspective on formulating poorly-water soluble compounds using wet media milling technology. Adv. Drug Deliv. Rev. 63, 427–440. https://doi.org/10.1016/j.addr.2010.12.007

Miladinov, V.D., Hanna, M.A., 1999. Physical and Molecular Properties of Starch Acetates Extruded with Water and Ethanol. Ind. Eng. Chem. Res. 38, 3892–3897.

https://doi.org/10.1021/ie990255p

Nagy, Z.K., Balogh, A., Drávavölgyi, G., Ferguson, J., Pataki, H., Vajna, B., Marosi, G., 2013. Solvent-Free Melt Electrospinning for Preparation of Fast Dissolving Drug Delivery System and Comparison with Solvent-Based Electrospun and Melt Extruded Systems. J. Pharm. Sci. 102, 508–517. https://doi.org/10.1002/jps.23374

Noyes, A.A., Whitney, W.R., 1897. The rate of solution of solid substances in their own solutions. J. Am. Chem. Soc. 19, 930–934. https://doi.org/10.1021/ja02086a003

Ogata, N., Lu, G., Iwata, T., Yamaguchi, S., Nakane, K., Ogihara, T., 2007. Effects of ethylene content of poly(ethylene-co-vinyl alcohol) on diameter of fibers produced by melt-electrospinning. J. Appl. Polym. Sci. 104, 1368–1375. https://doi.org/10.1002/app.25872

Savolainen, M., Heinz, A., Strachan, C., Gordon, K.C., Yliruusi, J., Rades, T., Sandler, N., 2007. Screening for differences in the amorphous state of indomethacin using multivariate visualization. Eur. J. Pharm. Sci. 30, 113–23. https://doi.org/10.1016/j.ejps.2006.10.010

Semjonov, K., Kogermann, K., Laidmäe, I., Antikainen, O., Strachan, C.J., Ehlers, H., Yliruusi, J., Heinämäki, J., 2017. The formation and physical stability of two-phase solid dispersion systems of indomethacin in supercooled molten mixtures with different matrix formers. Eur. J. Pharm. Sci. 97, 237–246. https://doi.org/10.1016/j.ejps.2016.11.019

Shalaev, E.Y., Zografi, G., 1996. How does residual water affect the solid-state degradation of drugs in the amorphous state? J. Pharm. Sci. 85, 1137–1141. https://doi.org/10.1021/js960257o

Shogren, R.L., 1996. Preparation, thermal properties, and extrusion of high-amylose

starch acetates. Carbohydr. Polym. 29, 57–62. https://doi.org/10.1016/0144-8617(95)00143-3

Sjöqvist, M., Gatenholm, P., 2005. The effect of starch composition on structure of foams prepared by microwave treatment. J. Polym. Environ. 13, 29–37. https://doi.org/10.1007/s10924-004-1213-8

Spiegel, S., Schmidt-Rohr, K., Boeffel, C., Spiess, H.W., 1993. 1H spin diffusion coefficients of highly mobile polymers. Polymer (Guildf). 34, 4566–4569. https://doi.org/10.1016/0032-3861(93)90166-8

Sun, D., Chang, C., Li, S., Lin, L., 2006. Near-field electrospinning. Nano Lett. 6, 839–842. https://doi.org/10.1021/nl0602701

Terife, G., Wang, P., Faridi, N., Gogos, C.G., 2012. Hot melt mixing and foaming of soluplus® and indomethacin. Polym. Eng. Sci. 52, 1629–1639. https://doi.org/10.1002/pen.23106

Tita, B., Fulias, A., Rusu, G., Tita, D., 2009a. Thermal behaviour of indomethacin-active substance and tablets kinetic study under non-isothermal conditions. Rev. Chim. 60, 1210–1215.

Tita, B., Fulias, A., Rusu, G., Tita, D., 2009b. Thermal behaviour of indomethacin-active substance and tablets kinetic study under non-isothermal conditions. Rev. Chim. 60, 1210–1215.

Vasconcelos, T., Sarmento, B., Costa, P., 2007. Solid dispersions as strategy to improve oral bioavailability of poor water soluble drugs. Drug Discov. Today 12, 1068–75. https://doi.org/10.1016/j.drudis.2007.09.005

Wei, C., Dong, J., 2013. Direct fabrication of high-resolution three-dimensional polymeric scaffolds using electrohydrodynamic hot jet plotting. J. Micromechanics Microengineering 23, 25017.

Williams, H.D., Trevaskis, N.L., Charman, S. a, Shanker, R.M., Charman, W.N., Pouton, C.W., Porter, C.J.H., 2013. Strategies to address low drug solubility in discovery and development. Pharmacol. Rev. 65, 315–499.

Zhu, Y., Shah, N., Waseem Malick, A., Infeld, M., McGinity, J., 2006. Controlled release of a poorly water-soluble drug from hot-melt extrudates containing acrylic polymers. Drug Dev. Ind. Pharm. 32, 569–583. https://doi.org/10.1080/03639040500528996

Figure captions

Figure 1. Schematic illustration of a melt electrospinning (MES) device with a heating system based on oil circulating through the jacket placed around the metal syringe. Arrow points out circulating heated oil and the direction of the collector movement.

Figure 2. Thermogravimetric analysis (TGA) (A) and differential scanning calorimetry (DSC) thermograms (B) of starting materials, physical mixtures (PMs) and melt-electrospun fibers (MSF). Key: γ-IND – indomethacin, SOL - Soluplus®, PM1 – the physical mixture of crystalline γ-IND and SOL at the weight ratio 1:3 (drug:polymer), PM2 – the physical mixture of amorphous IND and SOL at the weight ratio 1:3 (drug:polymer), PM3 – the PM1 stored at high RH (90%), MSF – melt-electrospun fibers prepared from PM3. The actual process temperature of MES (180 °C) is indicated with a solid line in the figure.

Figure 3. The SEM images of (A1) intact melt-electrospun fibers (MSF) of γ-IND and SOL at the weight ratio of 1:3 (drug to polymer), (A2) the corresponding ground MSFs, (B1) blank MSFs, and (B2) the corresponding ground blank MSFs. Key: γ-IND – indomethacin, SOL – Soluplus®.

Figure 4. X-ray powder diffraction (XRPD) patterns of starting materials, physical mixtures (PMs) and melt-electrospun fibers (MSF). Key: γ-IND – indomethacin, SOL – Soluplus®, PM1 – the physical mixture of crystalline γ-IND and SOL at the weight ratio 1:3 (drug:polymer), PM2 – the physical mixture of amorphous IND and SOL at the

weight ratio 1:3 (drug:polymer), PM3 – the PM1 stored at high RH (90%), MSF – melt-electrospun fibres prepared from PM3. All patterns are normalized and off-set for clarity.

Figure 5. Fourier Transform Infrared (FTIR) spectra of starting materials, physical mixtures (PMs) and melt-electrospun fibers (MSF) Key: γ-IND – indomethacin, SOL – Soluplus®, PM1 – the physical mixture of crystalline γ-IND and SOL at the weight ratio 1:3 (drug:polymer), PM2 – the physical mixture of amorphous IND and SOL at the weight ratio 1:3 (drug:polymer), PM3 – the PM1 stored at high RH (90%), MSF – melt-electrospun fibers prepared from PM3. All patterns are normalized and off-set for clarity.

Figure 6. Overlay of 1H-spectrum of physical mixture (PM) and melt-electrospun fibers (MSFs) (A) and ^{13}C CP-MAS-spectra of starting materials, physical mixtures (PMs) and melt-electrospun fibers (MSF) (B). Key: γ-IND – indomethacin, SOL – Soluplus®, PM1 – the physical mixture of crystalline γ-IND and SOL at the weight ratio 1:3 (drug:polymer), MSF – melt-electrospun fibers prepared from PM3 (the PM1 stored at high RH (90%).

Figure 7. *In vitro* dissolution profiles of γ-IND, physical mixtures (PMs) and melt-electrospun fibers (MSF) at the weight ratio 1:3 (drug:polymer) in pH 6.8 phosphate buffer (n=3). Key: γ-IND – indomethacin, PM1 – the physical mixture of crystalline γ-IND and SOL at the weight ratio 1:3 (drug:polymer), PM2 – the physical mixture of amorphous IND and SOL at the weight ratio 1:3 (drug:polymer), MSF – melt-electrospun fibers prepared from PM3. The error bars indicate the standard deviations (n = 3).

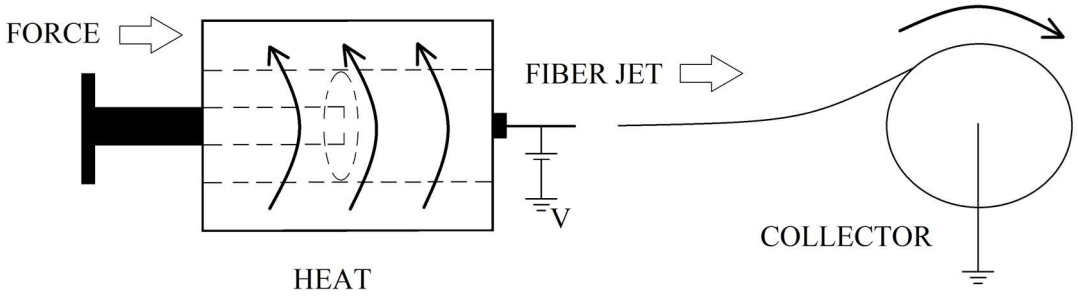

Figure 1.

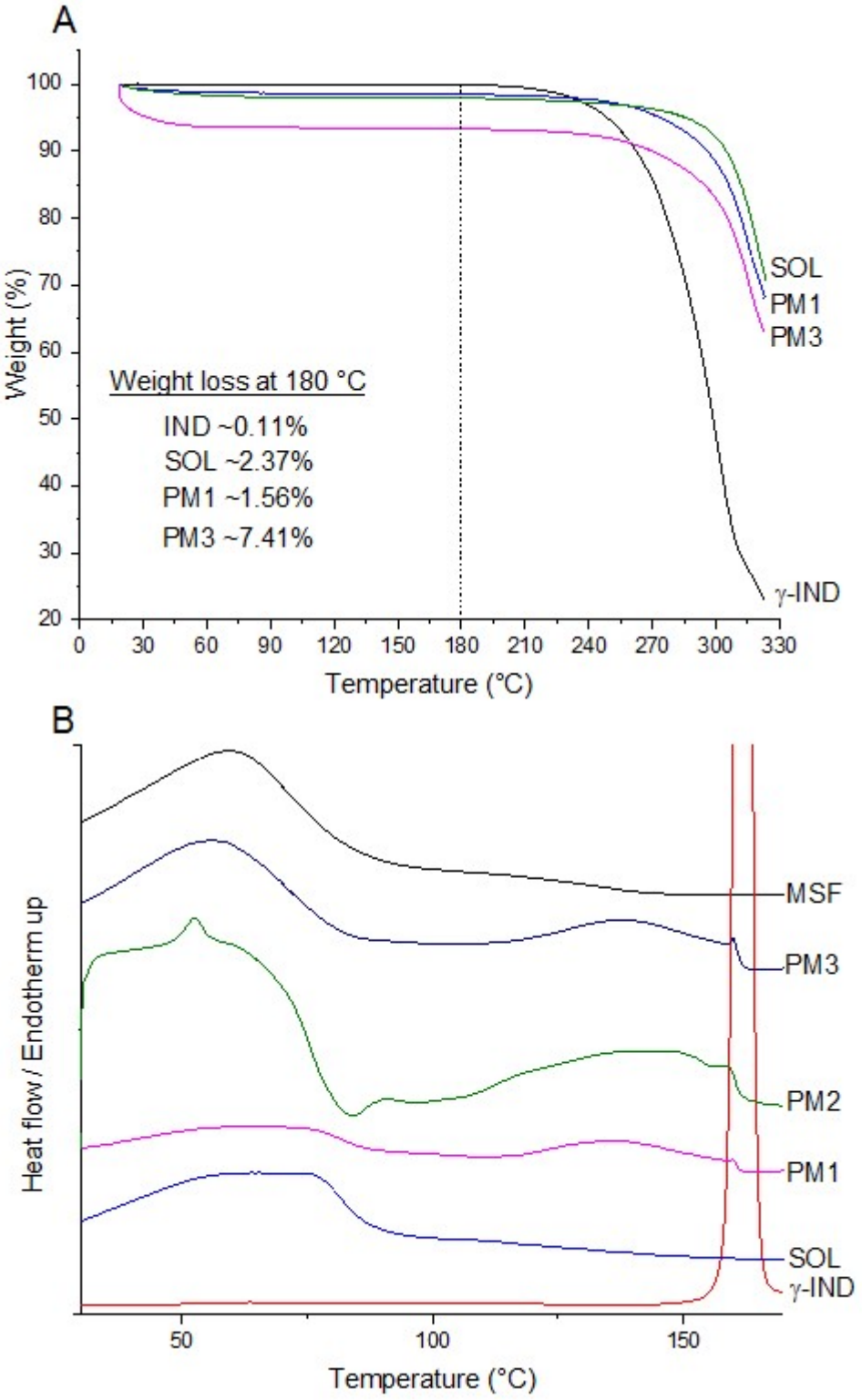
A
Weight (%)
Temperature (°C)
Weight loss at 180 °C
IND ~0.11%
SOL ~2.37%
PM1 ~1.56%
PM3 ~7.41%
SOL
PM1
PM3
γ-IND
B
Heat flow / Endotherm up
Temperature (°C)
MSF
PM3
PM2
PM1
SOL
γ-IND

Figure 2.

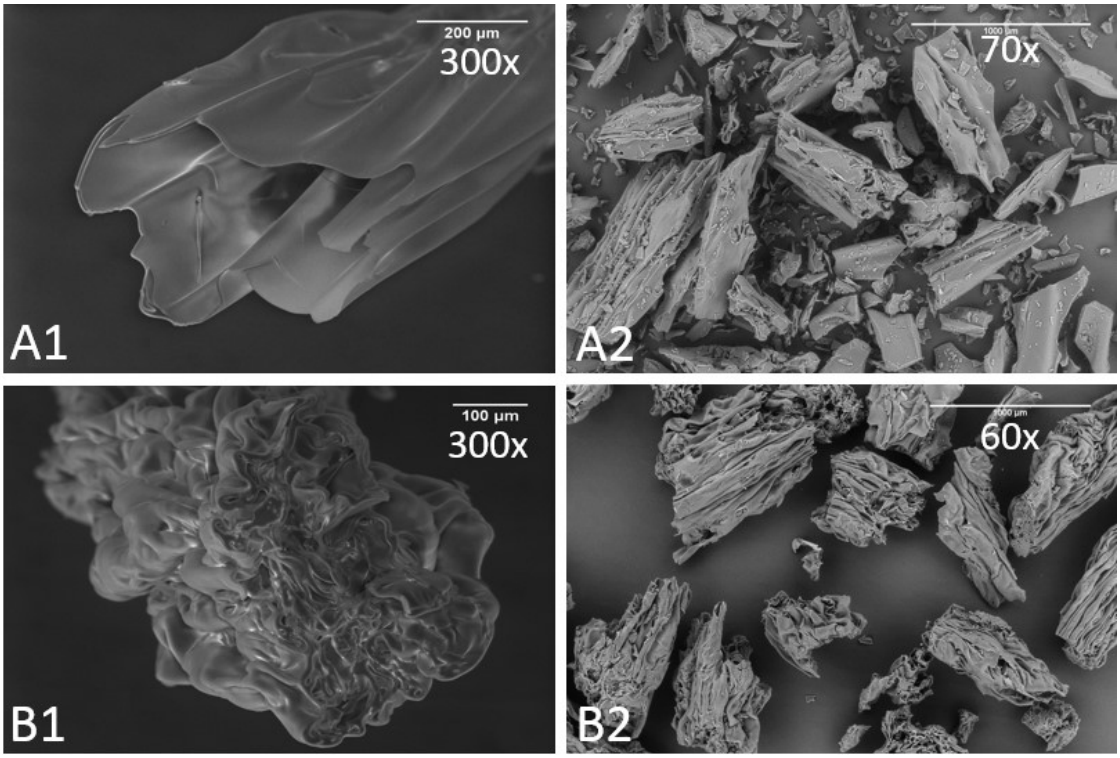

Figure 3.

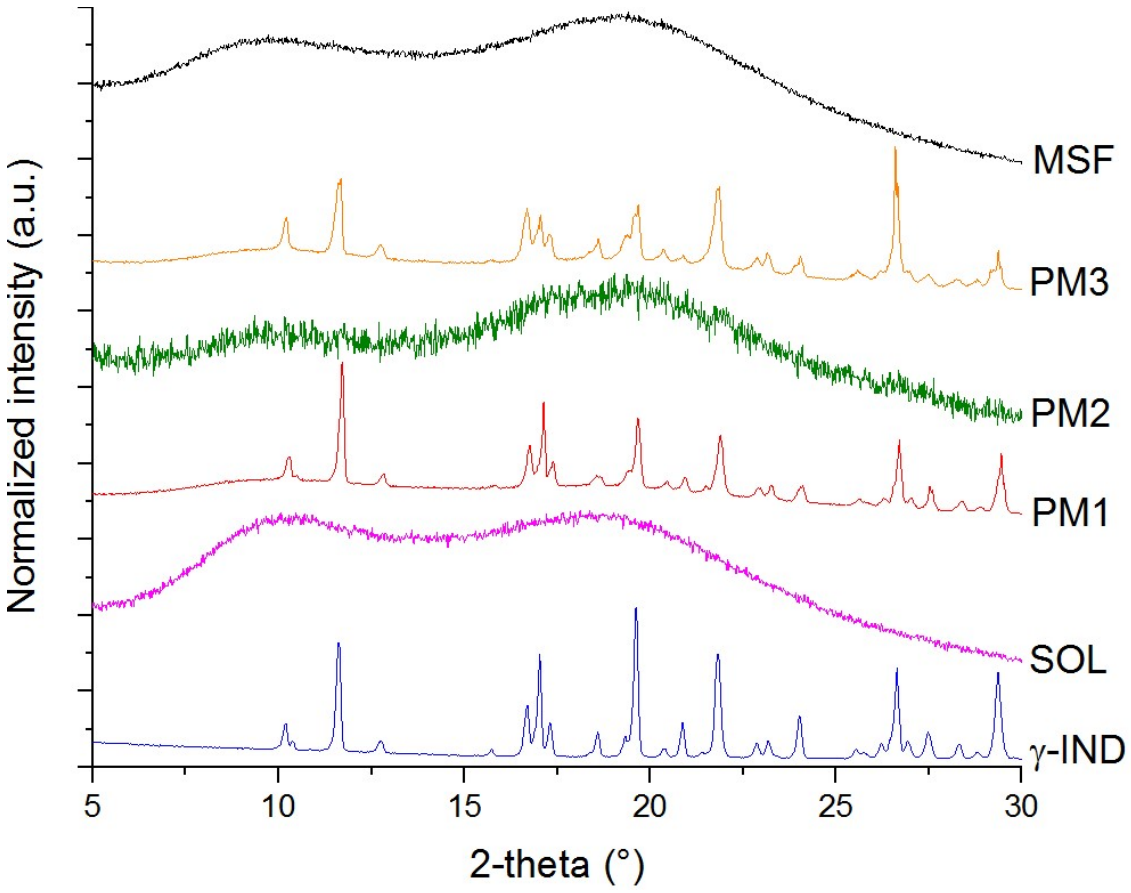
Normalized intensity (a.u.)
MSF
PM3
PM2
PM1
SOL
γ-IND
5
10
15
20
25
30
2-theta (°)

Figure 4.

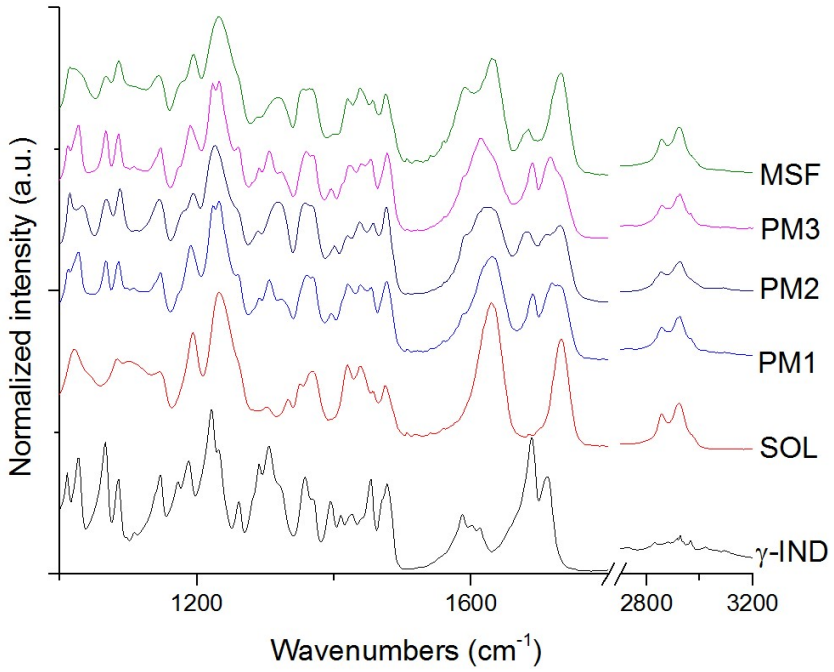
Normalized intensity (a.u.)
MSF
PM3
PM2
PM1
SOL
γ-IND
1200
1600
2800
3200
Wavenumbers (cm-1)

Figure 5.

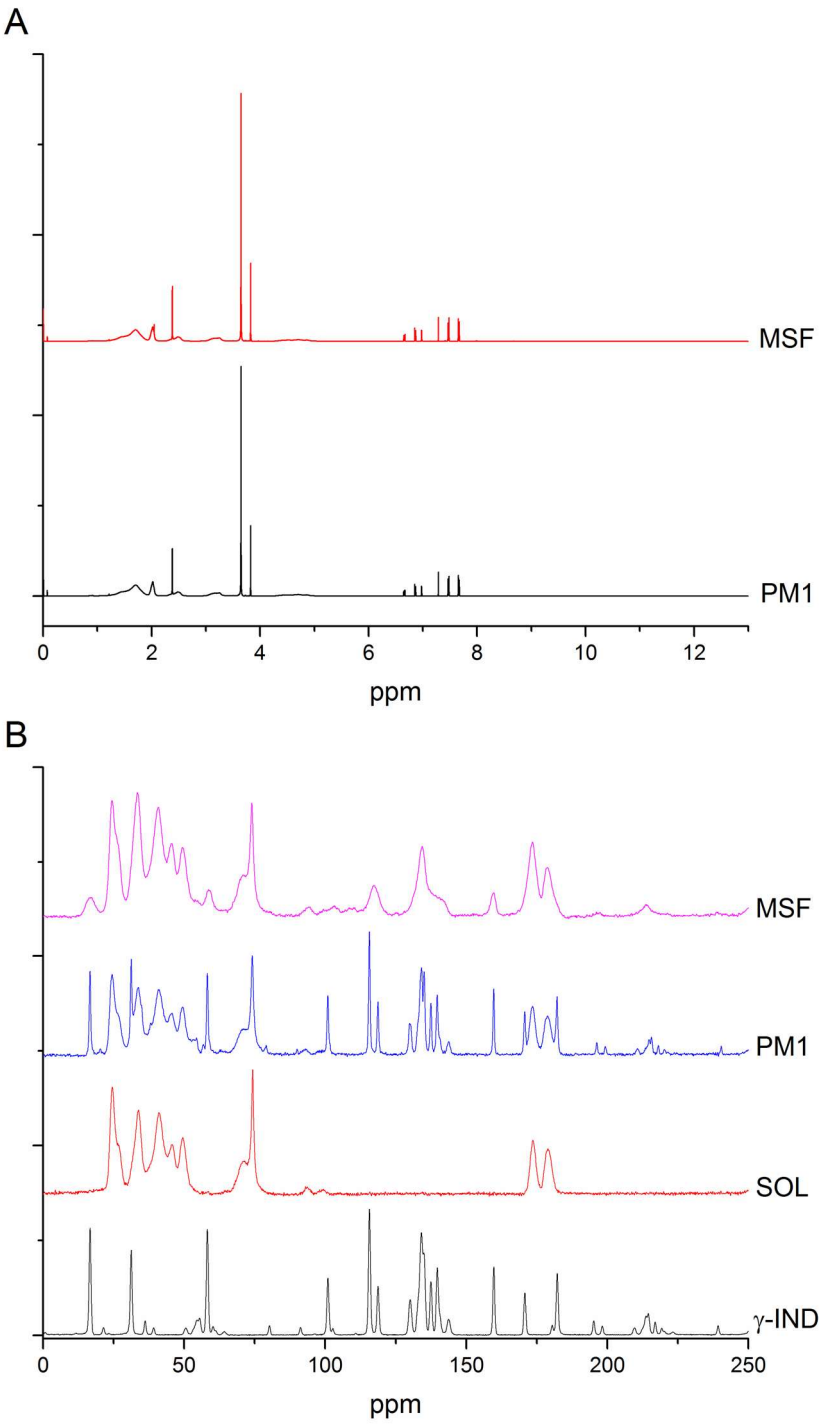
A
MSF
PM1
0
2
4
6
8
10
12
ppm
B
MSF
PM1
SOL
γ-IND
0
50
100
150
200
250
ppm

Figure 6.

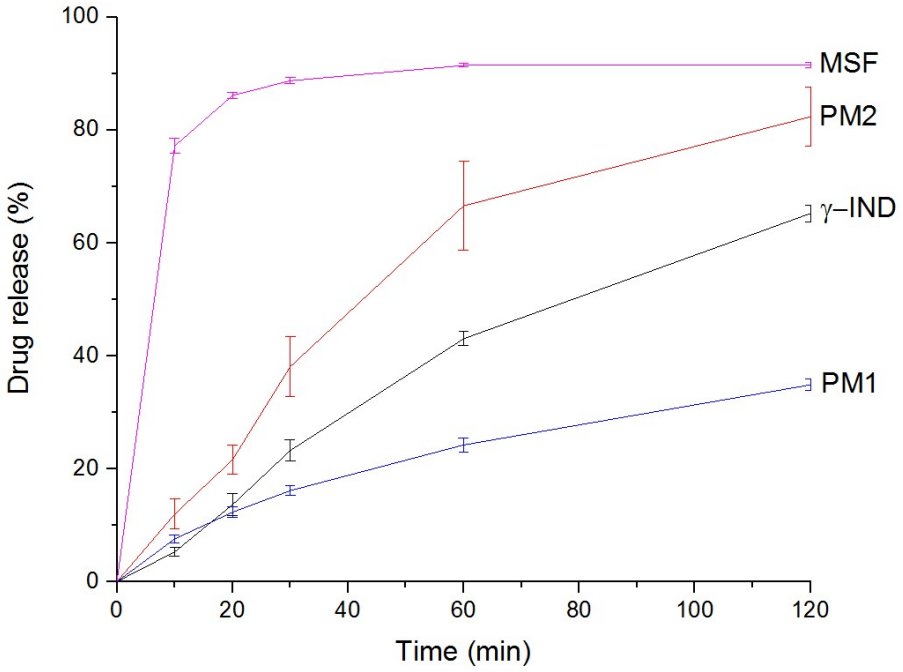

Figure 7.

Appendix. Near-infrared spectroscopy.

Method: Near-infrared spectroscopy (NIR) spectra (1200-2200 nm) were measured with AvaSpec-NIR256-2.2 (Avantes, Netherlands), equipped with 256 pixel inGaAs detector and tungsten halogen lamp as a light source (AvaLight-HAL). A reference spectrum was recorded with a Teflon background. The spectra were collected from 1100 to 2200 nm with a 30 ms integration time and the number of averaged scans per spectrum was 4. Each sample was measured in pentaplicate. Standard normal variate (SNV) correction and mean centering were used for pretreatment of the spectra.

NIR spectra were used to verify the moisture sorption on the PMs of IND and SOL. It can be clearly seen that the PMs stored at high RH (50% and 90%) sorb more water than the respective PMs stored at low RH (0%)(Appendix figure). The main differences can be observed in the NIR spectra at wavelengths that are related with water. Spectral features of water are overtones and combination bands at approximately 1400 (the first overtone related to O-H stretching vibration) and 1900-1950 nm (combination band of water) (Heinz et al., 2007; Savolainen et al., 2007).

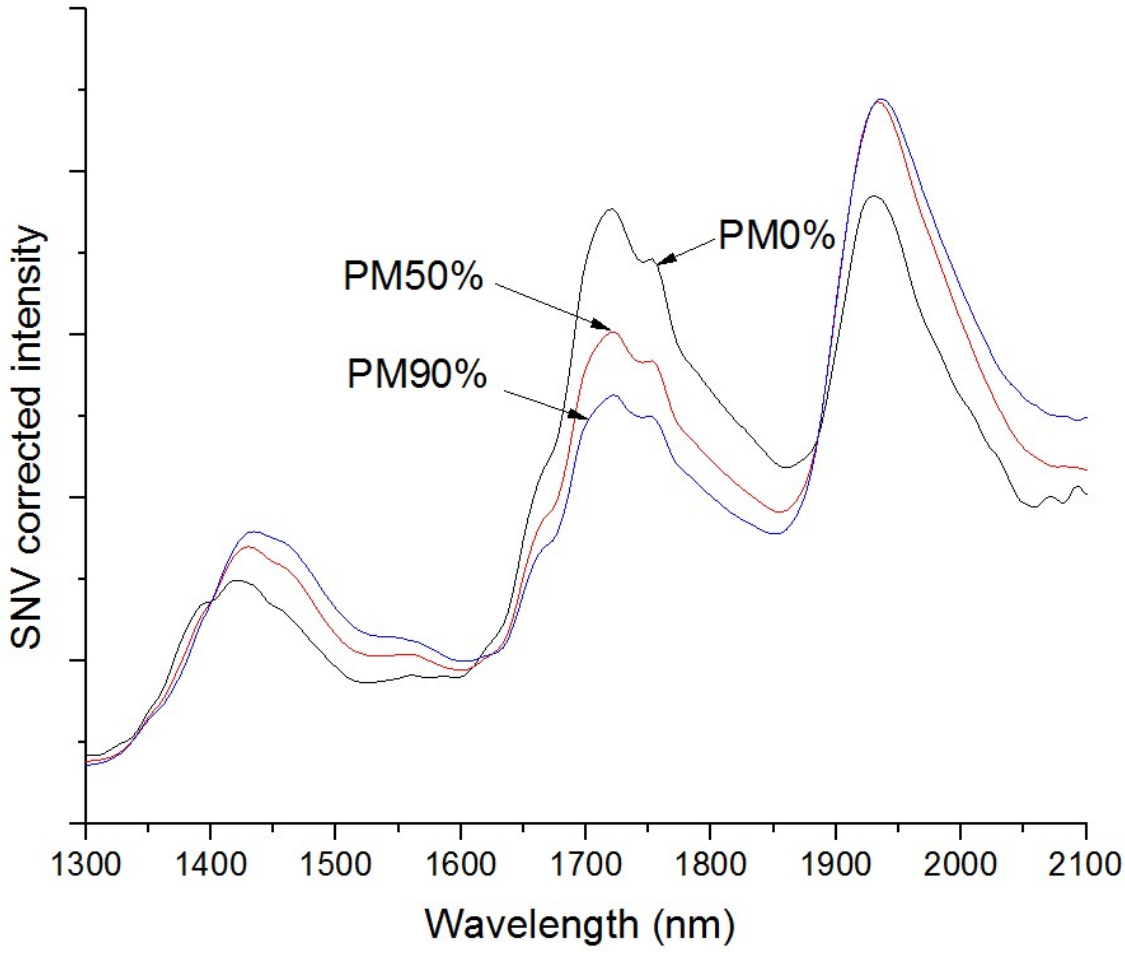

Appendix figure. Near-infrared (NIR) spectra of the physical mixture (PM) of crystalline IND and SOL at the weight ratio 1:3 (drug:polymer) stored at different RH.